HAb18G/CD147 Functions in Invasion and Metastasis of Hepatocellular Carcinoma

Jing Xu,[1] Hui-Yun Xu,[1] Qing Zhang,[1] Fei Song,[1] Jian-Li Jiang,[1] Xiang-Min Yang,[1] Li Mi,[1] Ning Wen,[1] Rong Tian,[1] Li Wang,[1] Hui Yao,[1] Qiang Feng,[1] Yang Zhang,[1] Jin-Liang Xing,[1] Ping Zhu,[2] and Zhi-Nan Chen[1]

[1]Cell Engineering Research Centre and Department of Cell Biology, State Key Laboratory of Cancer Biology and [2]Department of Clinical Immunology in Xijing Hospital, Fourth Military Medical University, Xi'an, China

Abstract

CD147 molecule is reported to be correlated with the malignancy of some cancers; however, it remains unclear whether it is involved in the progression of hepatocellular carcinoma (HCC). Here, we investigated the function of HAb18G/CD147, a member of CD147 family, and its antibodies, HAb18 and LICARTIN, in HCC invasion and metastasis. We observed that HAb18G/CD147 gene silence in HCC cells significantly decreased the secretion of matrix metalloproteinase (MMP) and the invasive potential of HCC cells ($P < 0.001$). MMP silence in HCC cells also significantly suppressed the invasion of the cells when cocultured with fibroblasts; however, its inhibitory effect was significantly weaker than that of both HAb18G/CD147 silence in HCC cells and that of MMP silence in fibroblasts ($P < 0.001$). Blocking the HAb18G/CD147 molecule on HCC cells with HAb18 monoclonal antibody resulted in a similar suppressive effect on MMP secretion and cell invasion, but with no significant effects on the cell growth. ^{131}I-labeled HAb18 F(ab′)$_2$ (LICARTIN), however, significantly inhibited the *in vitro* growth of HCC cells ($P < 0.001$). In an orthotopic model of HCC in nude mice, HAb18 and LICARTIN treatment effectively reduced the tumor growth and metastasis as well as the expression of three major factors in the HCC microenviroment (MMPs, vascular endothelial growth factor, and fibroblast surface protein) in the paracancer tissues. Overall, these results suggest that HAb18G/CD147 plays an important role in HCC invasion and metastasis mainly via modulating fibroblasts, as well as HCC cells themselves to disrupt the HCC microenviroment. LICARTIN can be used as a drug targeting to HAb18G/CD147 in antimetastasis and recurrence therapy of HCC. (Mol Cancer Res 2007;5(6):605–14)

Introduction

Tissue invasion and metastasis are important characteristics of malignant tumors, which always lead to tumor-associated death. Tumor metastasis depends on the properties of tumor cells and tumoral microenvironment that consists of stromal cells, extracellular matrix proteins, and other soluble factors such as cytokines (1). The interactions between tumor cells and tissue microenvironment are dynamic. Disruption of a single component in the tissue microenvironment may cause dramatic changes in the whole microenviroment and render the tissue susceptible to tumor invasion. Degradation and remodeling of extracellular matrix (the immediate pericellular environment of the cell) are necessary steps in local invasion (2). A major family of enzymes degrading extracellular matrix is matrix metalloproteinases (MMP). MMPs are secreted or membrane-anchored Zn^{2+}-dependent endopeptidases, which are capable of disrupting the basement membrane and cleaving the extracellular matrix components (3). A high level of MMPs is frequently found at the tumor-stroma interface, most of which is expressed by stromal cells rather than by tumor cells (4). In many tumors, MMP expression is mainly regulated by tumor-stroma interactions via tumor cell–associated extracellular MMP inducer (Emmprin, CD147), a highly glycosylated cell surface transmembrane protein that belongs to the immunoglobulin superfamily (5). CD147 is a cellular adhesion molecule involved in cell-cell and cell-extracellular matrix interactions. It can stimulate MMP production but does not affect the production of tissue inhibitor of metalloproteinases, the physiologic inhibitors for MMPs, hence modifying the collagenolytic balance toward MMP activation (6). CD147 expression is elevated on several human tumors and has been correlated with the malignancy in some cancers such as primary breast cancer and ovarian cancer, etc. (7-12). Despite the close correlation between CD147 expression and malignancy of some tumors, it is not clear whether CD147 has a functional role in tumor genesis and hepatocellular carcinoma (HCC) progression.

HCC is a highly malignant tumor characterized by rapid progression, easy metastasis, and frequent recurrence. We

previously developed an anti-HCC monoclonal antibody (mAb) HAb18 by using a cell suspension extracted from fresh human HCC tissues to immunize BALB/c mice and to prepare hybridoma (13-15). Its antigen, HAb18G, was identified by screening the HCC cDNA expression library and named HAb18G/CD147 for being homologous to CD147 (5, 16). In our previous studies, HAb18G/CD147 was found to be highly expressed on HCC cells and tissues. It was associated with tumor recurrence-free survival and could be used as a significant independent predictor of poor survival in HCC patients after tumor resection (17). For the HCC patients who received liver transplantation, CD147 was also found to be a significant predictor of tumor recurrence combined with the expression of CD34, a marker of microvessel density, and the expression of MMP-2 and MMP-9 in stromal compartment (18). The expression of tumor vascular endothelial growth factor (VEGF) was also positively correlated with that of CD147 (17). These findings suggest that CD147 may be involved in the tumor growth, invasion, and angiogenesis in HCC. HAb18 mAb, the HAb18G/CD147–specific antibody, and its bivalent fragment HAb18 F(ab′)$_2$ (Metuximab), could bind to HCC cells with high affinity. With flow cytometry analysis, HAb18 mAb exhibited a binding rate of 99.55% to human hepatoma cells, and using immunohistochemistry, it showed a positive HCC staining rate of 75% (39 of 52) with little cross-reaction to normal tissues (14, 16, 19). We had generated the ^{131}I-labeled Metuximab [trade name LICARTIN; generic name Iodine (^{131}I) Metuximab Injection] for in vivo injection. The pharmacokinetic characteristics and safety of the antibody and its radiolabeled conjugate had been determined both in vivo and in clinic (14, 16, 19-21). LICARTIN was approved to be a new drug for clinical therapy of primary HCC patients by China State Food and Drug Administration (no. S20050039) in April 2005. It has been proved to be safe and effective in treating primary HCC patients and can effectively prevent the recurrence of tumor and prolong the survival of advanced HCC patients after orthotropic liver transplantation (19, 22). In the present study, we further investigated the function of HAb18G/CD147 and its antibodies, HAb18 and LICARTIN, in HCC invasion and metastasis, and evaluated HAb18G/CD147 as a possible anti-HCC metastasis drug target.

Results

Effects of Silencing HAb18G/CD147 on HCC Cells

To investigate the role of HAb18G/CD147 in HCC invasion, RNA interference was used to knock down the expression of HAb18G/CD147 in two HCC cell lines, FHCC-98 (23) and MHCC97-H (24) cells. The HAb18G/CD147–specific (si-HAb18G) small interfering RNA (siRNA) and Silencer negative control siRNA (snc-RNA) were tested for their ability to specifically suppress HAb18G/CD147. Real-time quantitative PCR showed that the snc-RNA was incapable of inhibiting HAb18G/CD147 gene expression, whereas si-HAb18G could effectively decrease the mRNA expression of HAb18G/CD147 (Fig. 1A). These results were confirmed by Western blot and flow cytometry analyses. The protein expression of HAb18G/CD147 was obviously decreased in si-HAb18G–transfected

cells, but not in snc-RNA–transfected cells (snc-cells) 48 h after siRNA transfection (Fig. 1A). The flow cytometry also showed that at 4 days after the si-HAb18G transfection, the HAb18G/CD147 protein in HCC cells was still reduced by 44.9 ± 1.62%, whereas that in MHCC97-H cells was reduced by 40.1 ± 0.54%, respectively. These data show that si-HAb18G treatment effectively decreased HAb18G/CD147 expression in HCC cells.

The results of gelatin zymography showed that 48 h after transfection, MMP secretion was significantly decreased in FHCC-98 (Fig. 1B) and MHCC97-H cells (Fig. 2A) with an inhibitory rate of 64.6 ± 4.52% ($P < 0.001$) and 64.3 ± 4.72% ($P < 0.001$), respectively, compared with that in snc-cells. By in vitro invasion assay, it was found that the number of cells migrating through the filter was significantly decreased in the transfected FHCC-98 (Fig. 1D) and MHCC97-H cells (Fig. 2B) with an inhibitory rate of 80.1 ± 3.09% ($P < 0.001$) and 66.3 ± 4.51% ($P < 0.001$), respectively, compared with that of snc-cells, demonstrating a potential relationship between the decreased MMP secretion and the invasive capability of HCC cells.

To mimic in vivo tumor-stroma interaction in local microenvironment, HCC cells were cocultured with human fibroblasts and exhibited an enhanced invasive ability, with the trans-filter cell number 3.84 ± 0.67 times (FHCC-98) and 2.62 ± 0.51 times (MHCC97-H) higher than that when cultured alone (Figs. 1D and 2B). After silencing HAb18G/CD147 expression, the secretion of MMPs (MMP-2 and MMP-9) and the number of trans-filter cells in the coculture of FHCC-98 and fibroblasts were decreased by 59.0 ± 1.70% ($P < 0.001$) and 83.34 ± 0.83% ($P < 0.001$), respectively (Fig. 1B and D), whereas those in the coculture of MHCC97-H and fibroblasts were decreased by 62.5 ± 0.23% ($P = 0.001$) and 76.6 ± 1.68% ($P = 0.001$), respectively (Fig. 2A and B). These results suggest that down-regulation of HAb18G/CD147 expression may attenuate the invasive capability of HCC cells possibly by inhibiting MMP production.

To further confirm the above inference, the effects of MMP-2 and MMP-9 gene cosilence on invasion were examined in four groups of coculture cells to determine whether MMPs produced by HCC cells or by fibroblasts play a more important role in invasion. The four groups were group 1 snc-HCC cells cocultured with snc-fibroblasts (negative control cells), group 2 si-MMP2/9-HCC cells cocultured with snc-fibroblasts, group 3 snc-HCC cells cocultured with si-MMP2/9 fibroblasts, and group 4 si-MMP2/9-HCC cells cocultured with si-MMP2/9 fibroblasts. The in vitro invasion assay showed that cells migrating through the filter in all the latter three groups (groups 2, 3, and 4) were significantly decreased compared with those in group 1 ($P < 0.001$ for each; Fig. 3A). However, significant differences were also found between any two groups of the latter three groups ($P < 0.001$ for each two groups, but $P = 0.004$ for groups 3 and 4 of MHCC97-H cells). The inhibitory effect on invasion in group 2 (FHCC-98, 20.2 ± 2.50%; MHCC97-H, 29.3 ± 1.94%) was significantly weaker than that both in group 3 (FHCC-98, 54.9 ± 1.94%, $P < 0.001$; MHCC97-H, 62.8 ± 5.69%, $P < 0.001$) and in group 4 (FHCC-98, 84.7 ± 2.24%, $P < 0.001$; MHCC97-H, 76.6 ± 5.85%, $P < 0.001$). The inhibitory effects on MMP secretion showed

a similar trend by gelatin zymography ($P < 0.001$, Fig. 3B). Compared with the silence of HAb18G/CD147 in HCC cells, the silence of MMPs in HCC cells (group 2) exhibited a significant weaker suppression of MMP secretion ($P < 0.001$) and cell invasion ($P < 0.001$) in the coculture. These results suggest that HAb18G/CD147 regulates HCC cell invasion via the modulation of MMP production and the modulation of fibroblasts plays a more important role.

Effects of Blocking HAb18G/CD147 by Its Antibody on HCC Cells

The competitive binding test was done to determine the blocking efficiency of HAb18 mAb on HAb18G/CD147 in HCC cells. RPE-labeled anti-CD147 antibody presented a gated positive binding rate of $96.12 \pm 2.18\%$ to FHCC-98 and $95.65 \pm 2.70\%$ to MHCC97-H cells. However, after HCC cells were incubated with HAb18 mAb, RPE-labeled anti-CD147 antibody presented only a rate of $1.24 \pm 0.46\%$ to FHCC-98 and $1.29 \pm 0.37\%$ to MHCC97-H cells, which were close to those of the blank control cells ($0.59 \pm 0.36\%$ and $0.76 \pm 0.34\%$; Figs. 1C and 2C). These results suggest that HAb18 mAb effectively bind to and block HAb18G/CD147 molecule on HCC cells with a relatively high affinity.

We then determined the effects of blocking HAb18G/CD147 by HAb18 mAb on HCC cells. As shown in Fig. 1B and D, HAb18 mAb treatment of FHCC-98 cells cultured alone or cocultured with fibroblasts decreased MMP secretion by $59.9 \pm 3.87\%$ ($P < 0.001$) or $63.1 \pm 3.54\%$ ($P < 0.001$) and the trans-filter cell number by $82.6 \pm 2.92\%$ ($P < 0.001$) or $86.0 \pm 1.55\%$ ($P < 0.001$), respectively, compared with those in negative control cells treated with an unrelated control mAb, anti-Japanese encephalitis virus mAb (anti-JEV mAb). Similar results were obtained in MHCC97-H cells. After HAb18 mAb treatment of the cells cultured alone or cocultured with fibroblasts, the MMP secretion was decreased by $71.0 \pm 8.08\%$ ($P < 0.001$) or $67.7 \pm 2.75\%$ ($P < 0.001$), respectively, and the trans-filter cell number was decreased by $69.0 \pm 3.73\%$ ($P < 0.001$) or $78.0 \pm 1.42\%$ ($P = 0.001$), respectively, compared with those in negative control cells (Fig. 2A and B). These results show that anti-HAb18G/CD147 mAb treatment decreases HCC invasion and MMP secretion.

Effects of HAb18 mAb and LICARTIN on HCC Cell Growth

To determine whether the antibody treatment affected the growth of HCC cells, we treated the cells with anti-JEV mAb (negative control), HAb18 mAb, ^{131}I, and LICARTIN, respectively, and counted the live cell number at different time points. Results showed that negative control mAb did not influence the cell growth (FHCC-98, $P = 0.863$; MHCC97-H, $P = 0.928$) compared with blank control. HAb18 mAb treatment slightly but not significantly inhibited the cell growth (FHCC-98, $P = 0.202$; MHCC97-H, $P = 0.273$), compared with the negative control, whereas ^{131}I and LICARTIN treatments exerted significant inhibitory effects on the cell growth (FHCC-98, $P_{131\text{iodine}} = 0.049$, $P_{\text{LICARTIN}} < 0.001$; MHCC97-H, $P_{131\text{iodine}} = 0.004$, $P_{\text{LICARTIN}} < 0.001$; Fig. 4). For FHCC-98 cells, the doubling time calculated was 25.73 ± 0.16 h of the

blank control and 26.01 ± 0.60 h, 26.89 ± 0.55 h, 27.52 ± 0.35 h, and 29.26 ± 0.41 h, respectively, of the negative control mAb−, HAb18 mAb−, ^{131}I-, and LICARTIN-treated cells. For MHCC97-H cells, the doubling time was 30.82 ± 0.53 h of the blank control and was 30.55 ± 0.48 h, 31.52 ± 1.00 h, 33.66 ± 0.78 h, and 40.41 ± 1.54 h, respectively, of the negative control mAb−, HAb18 mAb−, ^{131}I-, and LICARTIN-treated cells. The findings that HAb18 mAb treatment had no significant effect on the growth of HCC cells and LICARTIN treatment exhibited the most obvious effects on the doubling time indicate that the influence of 1-h LICARTIN treatment on the cell growth may be due to the killing effects of ^{131}I, which is maintained on the cell surface via the specific recognition and binding of the conjugated antibody to HAb18G/CD147 on HCC cells.

Inhibitory Effects of HAb18 mAb and LICARTIN on HCC in an Animal Model

To investigate whether HAb18 mAb and LICARTIN have the *in vivo* anti-HCC growth and metastasis potential, we used an orthotopic model of HCC in nude mice. Animals were randomized to receive negative control mAb, HAb18 mAb, low-dose or high-dose of LICARTIN, or 0.9% NaCl solution. One month posttreatment, no significant difference in the body weight of mice was found among the five groups ($P = 0.477$). The tumor-related adverse effects, such as pachylosis, anorexia, and depression, appeared obviously earlier in the control groups than those in the treatment groups. The anorexia was observed in the LICARTIN treatment groups, but soon disappeared after the treatment was completed. No death occurred in any of the five groups during the observation period.

All the mice were sacrificed 1 month postimplantation and the implanted tumors from each mouse were removed and measured for tumor size. Significant differences of tumor size were found among the five groups ($P < 0.001$). There was no significant difference between the blank control and negative control group ($P = 0.343$), whereas the tumor growth was significantly inhibited in HAb18 mAb−, low-dose and high-dose LICARTIN treatment groups with an inhibitory rate of 34.34% ($P < 0.001$), 60.01% ($P < 0.001$), and 82.31% ($P < 0.001$), respectively, compared with that in the negative control group. High-dose LICARTIN exhibited the strongest inhibitory effect (Fig. 5A and B). According to Chinese Pharmacopeia Instruction for New Drug Development, an antitumor drug is considered to be effective when its inhibitory rate of tumor growth is above 30%. By this standard, HAb18 mAb and LICARTIN are effective antitumor agents in the animal model.

We also analyzed the effects of these treatments on HCC metastasis. The metastases in all the mice were counted and verified by H&E staining (Fig. 5C). Single or fused small metastases were found only in the liver, whereas no metastases were found in other examined organs of all mice with metastasis. In the treatment group, large necrosis in the local tumor was found and cell debris and inflammatory cell infiltration could be seen in the necrosis tissues. No pathologic changes were seen in the main organs and paracancer liver (data not shown). Metastasis was observed in all mice of the two control groups, but only in three (33.33%), one (16.67%), and zero mice, respectively, in HAb18 mAb, low-dose LICARTIN group, and high-dose LICARTIN group. Significant differences
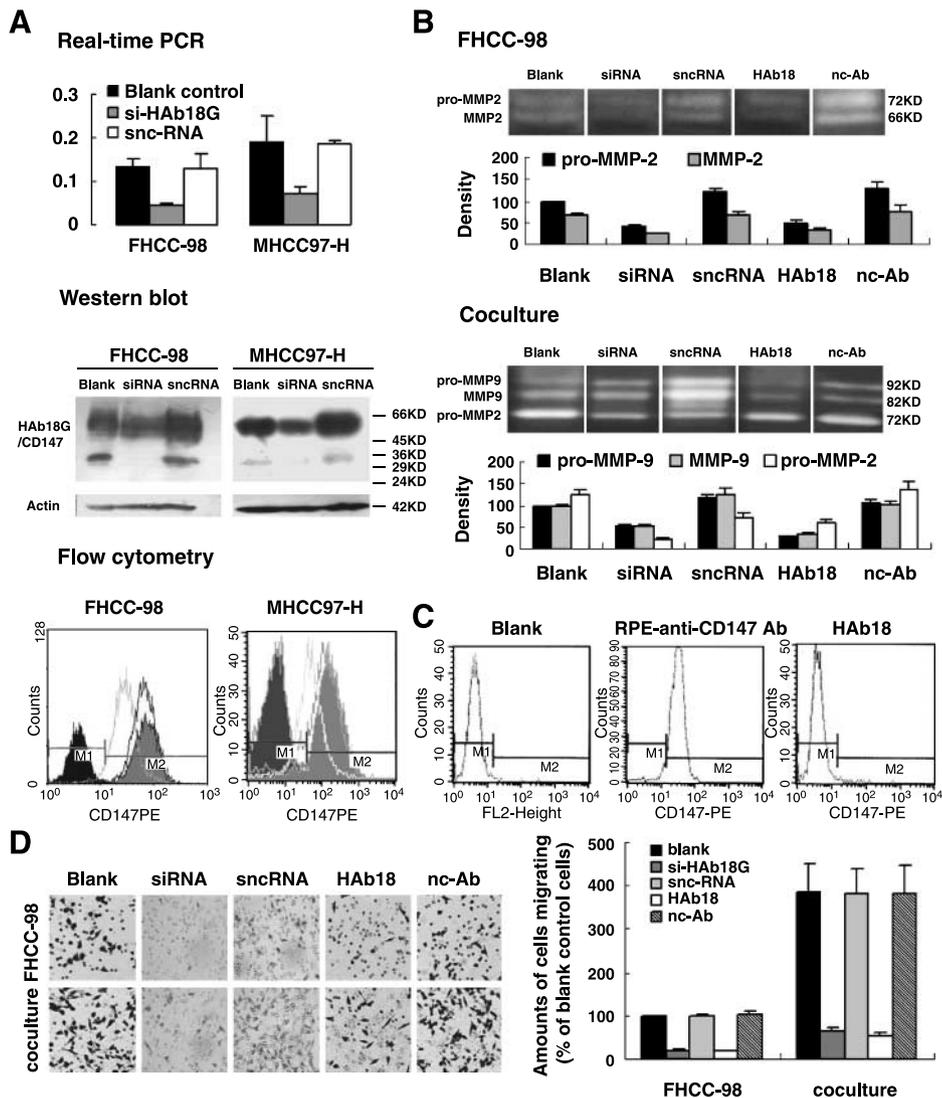
FIGURE 1. Silencing or blocking HAb18G/CD147 in FHCC-98 cells inhibited the cellular secretion of MMPs and the invasive potential. **A.** Forty-eight hours after si-HAb18G or snc-RNA transfection of FHCC-98 or MHCC97-H cells, HAb18G/CD147 expression levels were examined by real-time quantitative PCR, Western blot, and flow cytometric analysis (*solid black columns,* negative control; *gray columns,* transfected with si-HAb18G; *black columns,* transfected with snc-RNA; *solid gray columns,* blank control). **B.** Gelatin zymography analysis of MMP secretion in FHCC-98 cells cultured alone (*FHCC-98*) or cocultured with fibroblasts (*Coculture*). Top, representative image; bottom, the gray scale analysis of at least three independent experiments. Columns, mean; bars, SD. **C.** The competitive binding of HAb18 mAb to HAb18G/CD147 on FHCC-98 cells was analyzed by flow cytometry. **D.** *In vitro* tumor cell invasive capability assay of FHCC-98 cells cultured alone or cocultured with fibroblasts. Left, representative photos showing the cell density on the filter. Right (*graph*), quantitative analyses for the cells migrating through the filter in three independent experiments. Columns, mean; bars, SD.

of tumor metastasis were found among the five groups ($P < 0.001$). There was no significant difference between the blank control and negative control group ($P = 0.578$), whereas the metastasis was significantly suppressed in HAb18 mAb ($P = 0.003$), low-dose LICARTIN treatment group ($P = 0.001$), and high-dose LICARTIN treatment group ($P = 0.001$), respectively, compared with that in the negative control group. High-dose LICARTIN exhibited the strongest inhibitory effect on HCC metastasis in this model (Table 1).

When examined by immunohistochemistry, HAb18G/CD147 was found to be highly expressed in the implanted tumors and in the metastases (Fig. 5C). To investigate the effects of anti-HAb18G/CD147 mAb treatments on HCC microenvironments, we determined fibroblast distribution, MMP-2, and VEGF expression in liver. The fibroblast surface protein (FSP) was used to trace fibroblast distribution. By image gray scale analysis, the staining intensity of FSP in the treatment groups was significantly weaker than that in the two control groups ($P < 0.001$ for both; Fig. 5C and D), suggesting a decreased FSP expression or paracancer fibroblasts after

antibody treatments. Similar results of MMP-2 and VEGF were obtained as shown in Fig. 5C and D, indicating that anti-HAb18G/CD147 treatments decrease the expression of MMP-2 and VEGF in HCC microenvironment, which is possibly related to the decreased fibroblasts around the tumors.

Discussion

Our previous reports suggested that HAb18G/CD147 was an HCC-associated antigen and was possibly related to HCC invasion *in vitro* (25-27). In the present study, we examined the role of HAb18G/CD147 in HCC invasion and metastasis *in vitro*, and in an orthotopic model of HCC in nude mice. Our data suggest that HAb18G/CD147 is involved in multiple processes in HCC invasion and metastasis. Knocking down or blocking HAb18G/CD147 in two HCC cell lines inhibits the invasive potential of these tumor cells, which may be due to the following mechanisms. HAb18G/CD147 could regulate HCC invasive capability through MMP (mainly MMP-2 and MMP-9) production. When HCC cells were cultured alone, si-HAb18G and HAb18 mAb decreased the autocrine
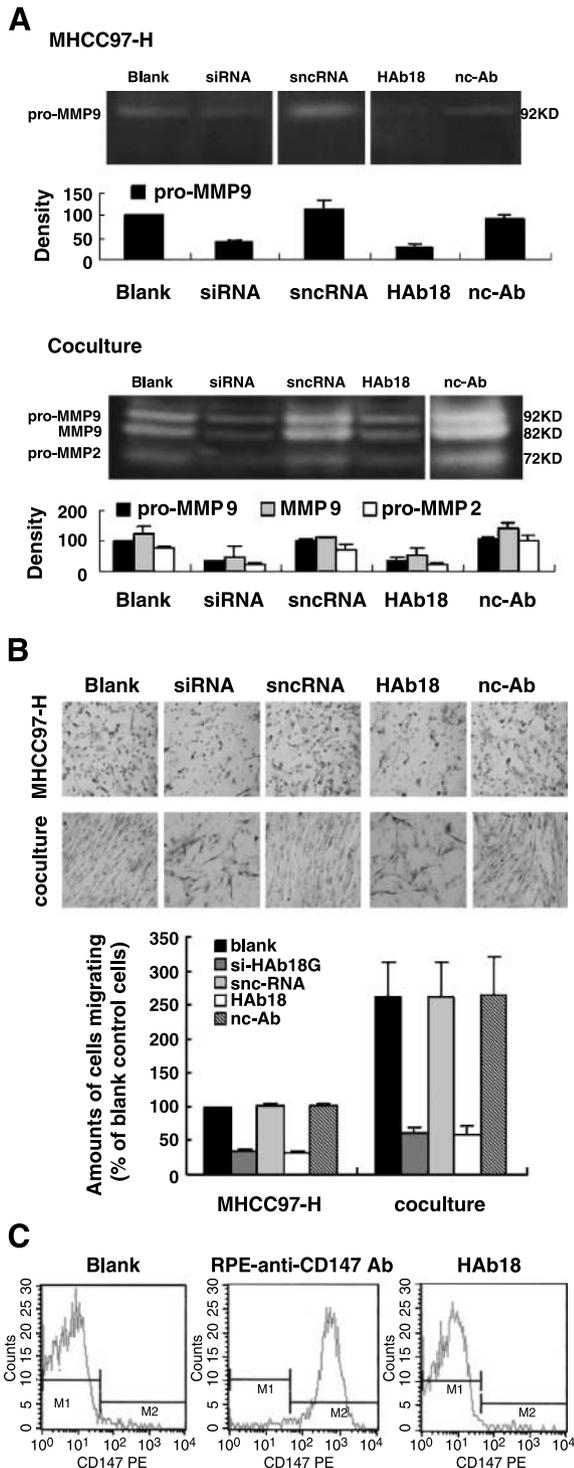
FIGURE 2. Silencing or blocking HAb18G/CD147 in MHCC97-H cells inhibited the cellular secretion of MMPs and the invasive potential. **A.** Gelatin zymography analysis of MMP secretion in MHCC97-H cells cultured alone (*MHCC97-H*) or cocultured with fibroblasts (*Coculture*). Top, a representative image; bottom, gray scale analysis of at least three independent experiments. Columns, mean; bars, SD. **B.** *In vitro* tumor cell invasive capability assay of MHCC97-H cells cultured alone or cocultured with fibroblasts. Top, cell density on the filter; bottom, quantitative analyses for the cells migrating through the filter in three independent experiments. Columns, mean; bars, SD. **C.** The competitive binding of HAb18 mAb to HAb18G/CD147 on MHCC97-H cells was analyzed by flow cytometry.

production of MMPs by inhibiting cellular expression of HAb18G/CD147. When HCC cells were cocultured with fibroblasts, a tumor-stroma interaction system mimicking *in vivo* situation, HCC cells exhibited an enhanced invasive ability, suggesting that some interactions between cancer cells and fibroblasts can promote the tumor invasion. Down-regulating or blocking tumor cell HAb18G/CD147 significantly decreased this invasive potential of HCC cells and also significantly attenuated the MMP production. MMP-2 and MMP-9 were previously reported to be involved in human hepatic tumorigenesis and metastasis (28). In this study, MMP (*MMP-2* and *MMP-9*) gene silence in HCC cells also significantly inhibited the invasion in the coculture system, but its inhibitory effects were significantly weaker than not only HAb18G/CD147 silence in HCC cells but also MMP silence in fibroblasts. These results suggest that HAb18G/CD147 plays a role in HCC invasion via regulation of MMP production by both tumor cells and surrounding fibroblasts, thus influencing the balance of tumor microenvironment, and the modulation of that by fibroblasts was more critical in the process. Our previous study also showed that HAb18G/CD147 was involved in tumor metastasis and invasion as a signal transduction molecule by regulating Ca^{2+} inflow (25, 27). All these findings show that HAb18G/CD147 may play some important roles in HCC progression, including adhesion, migration, and enzymes degradation.

HAb18G/CD147 in *in vivo* study also was found to play a critical role in HCC invasion and metastasis. Treatment of HCC tumor-bearing mice with anti-HAb18G/CD147 antibodies significantly decreased tumor metastasis, which may be to the results of the decreased host fibroblasts around HCC tissues and the expression of MMP-2 and VEGF in the paracancer tissues. Tumor-associated fibroblasts are known as the major effector population in stroma interacting with CD147 on tumor cells. The tumor-associated fibroblast-tumor cell interaction promotes the secretion of MMPs and some active cytokines, leading to tumor proliferation and metastasis. However, the mechanism by which CD147 interacts with tumor-associated fibroblasts in modulating MMP production remains unclear. It may be mediated by reducing either cellular MMP secretion or/and the number of fibroblasts. Our *in vitro* coculture data of gelatin zymography suggest a reduced cellular MMP secretion and the *in vivo* data of immunohistochemistry suggest a reduced number of fibroblasts, which may result from the inhibited proliferation or chemotaxis of fibroblasts.

The anti-HAb18G/CD147 antibody treatment also achieved a significant suppressive effect on HCC growth *in vivo*. However, *in vitro*, no significant inhibitory effects of HAb18 mAb were found on HCC cell doubling time, which was consistent with Chung's report (29) that down-regulating CD147 expression on breast cancer cells had little effect on the viability of the cells cultured in an anchorage-dependent growth model. Taken together with the *in vivo* inhibitory effects of HAb18 mAb on MMPs and VEGF expression in paracancer tissues, the significantly suppressive efficacy of HAb18 mAb treatment on HCC growth *in vivo* can be partially attributed to the regulation of MMP production in tumor microenvironment by HAb18G/CD147, as MMPs are considered to contribute to the tumor growth *in vivo* (30). The significant inhibitory effects of

A

B
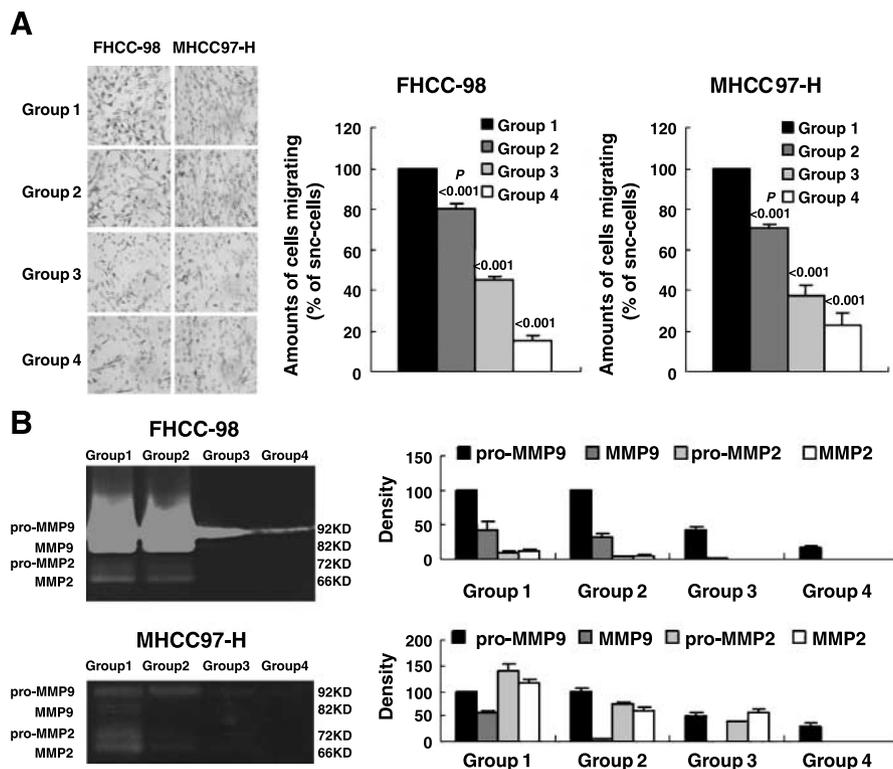
FIGURE 3. MMP gene silence suppressed the cell invasion in the coculture. **A.** *In vitro* cell invasive capability assay in four groups of cocultured cells. Group 1, snc-HCC cells cocultured with snc-fibroblasts (negative control); group 2, si-MMP2/9-HCC cells cocultured with snc-fibroblasts; group 3, snc-HCC cells cocultured with si-MMP2/9-fibroblasts; group 4, si-MMP2/9-HCC cells cocultured with si-MMP2/9-fibroblasts. Left photos, cell density on the filter; middle and right (*graph*), quantitative analyses for the cells migrating through the filter in three independent experiments. Columns, mean; bars, SD. **B.** Gelatin zymography analysis of MMP secretion in the above groups of cells mentioned in (**A**). Left, representative images; right, gray scale analysis of three independent experiments. Columns, mean; bars, SD.

LICARTIN on HCC cell growth *in vitro* can be attributed to the killing effects of ^{131}I, which is maintained on the cell surface due to the specific recognition and binding of the conjugated antibody. *In vivo*, LICARTIN presented stronger efficacy of growth suppression than HAb18 mAb. This efficacy may come from both the function of HAb18G/CD147 molecule and the killing effect of radionuclide.

Tumor progression is a multistep process. Many factors involved in this process can be used as potential targets for tumor therapy. MMPs are believed to be one of such targets and some researches on MMP inhibitors have been conducted. Although some promising results using MMP inhibitors to suppress tumor invasion have been reported, MMP inhibitors are not effective in treating patients with advanced cancer in most cases (31-33). According to Hess et al. (34) and Chen et al. (35) this failure can be explained by the findings that some MMPs may play a role in early stages of cancer and that metastatic cascade is already fully played out before MMP inhibition has a chance to take effect. However, as this study indicates that HAb18G/CD147 can regulate MMP production, blocking HAb18G/CD147 on HCC cells can suppress the metastatic cascade at the upstream of MMPs in HCC microenvironment and can be a new strategy for the molecularly targeted treatment of HCC.

In conclusion, our present work shows that HAb18G/CD147 play an important role in HCC invasion and metastasis mainly via regulating fibroblasts, as well as tumor cells themselves to disrupt the HCC microenvironment and can be a drug target for preventing HCC metastasis. Its antibodies, especially LICARTIN, can effectively inhibit HCC tumor growth and metastasis *in vivo* and may be used as a promising drug for antimetastasis and recurrence therapy of HCC.

Materials and Methods

Cell Lines

Two HCC cell lines used were FHCC-98 and MHCC97-H cells, with highly invasive ability and positively expressing HAb18G/CD147. FHCC-98 cell was originated from the tumor tissues of a 39-year-old Chinese male HCC patient and conserved in our laboratory. MHCC97-H cell was supplied by Liver Cancer Institute of Fudan University (Shanghai, China). Human embryo pulmonary fibroblast-1 was purchased from Chinese Academy of Medical Sciences.

RNA Interference

si-HAb18G (5′-GUUCUUCGUGAGUUCCUCtt-3′, 3′-dTd-TCAAGAAGCACUCAAGGAG-5′), si-MMP-2 (5′-GGGUGC-CUAUUACCUGAAGtt-3′, 3′-ttCCCACGGAUAAUGGACU-UC-5′), and si-MMP-9 (5′-GAUGCGUGGAGAGUCGAAAtt-3′, 3′-ttCUACGCACCUCUCAGCUUU-5′) were synthesized by Ambion, Inc. HCC cells were transfected with siRNA using LipofectAMINE 2000 reagent according to the manufacturer's instruction (Invitrogen). Silencer negative control 1 siRNA (Ambion) was used as negative control under similar conditions.

Real-time Quantitative PCR and Data Analysis

Forty-eight hours after siRNA transfection, the total RNA was extracted from the cells with TRIzol reagents (Invitrogen) and reversely transcribed into cDNA with ReverTra Ace-α kit (TOYOBO). The Taqman probes were labeled with 6-carboxy-fluorescein (FAM) at the 5′ end and 6-carboxytetramethylyhod-amine (TAMRA) at the 3′ end and hybridized to a sequence located between the PCR primers. All primers and probes were synthesized by Shanghai Sangon Co. as follows: HAb18G/
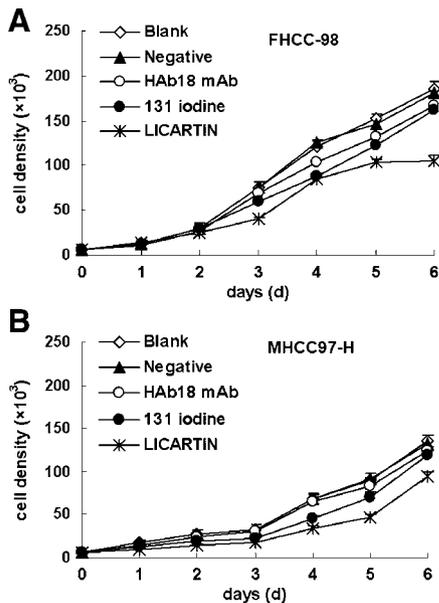
FIGURE 4. Effects of HAb18 mAb, ^{131}I, and LICARTIN on HCC cell growth. Cell growth curve of FHCC-98 (**A**) and MHCC97-H (**B**) cells untreated (*Blank*) or treated with negative control mAb (*Negative*), HAb18 mAb, [131]I (*131 iodine*), and LICARTIN, respectively.

CD147, forward primer 5′-TCGCGCTGCTGGGCACC-3′; reverse primer 5′-TGGCGCTGTCATTCAAGGA-3′; and TaqMan probe 5′ FAM-CCGGGGCTGCCGGCA-CAGTC-TAMRA-3′. β-Actin (control): forward primer 5′-CCCAGCCATGTACGTTGCTA-3′; reverse primer 5′-TCACCGGAGT-CCATCACGAT-3′; and TaqMan probe 5′ FAM-CGCCTCTGGCCGTACCACTG-TAMRA-3′. Real-time quantitative PCR was preformed with MiniOpticon system (Bio-Rad). The conditions for PCR were one cycle of 94°C for 4 min, 45 cycles of 94°C for 20 s, 58°C for 20 s, and 72°C for 20 s. All PCR reactions were done in triplicate. The cycle threshold value (C_T) was determined as the point at which the fluorescence exceeded a preset limit by the instrument's software (Opticon monitor, version 3.1). The relative expression of HAb18G/CD147 mRNA was calculated by the ΔC_T method (where ΔC_T is the value calculated by subtracting the C_T value of β-actin from the C_T value of HAb18G/CD147 in each samples). The amount of HAb18G/CD147 relative to β-actin mRNA was expressed as $2^{-(\Delta C_T)}$.

Western Blot

Forty-eight hours after siRNA transfection, HCC cells were harvested in a lysis buffer and equal amount of cellular proteins were subjected to SDS-PAGE (10%) separation. Proteins were transferred to polyvinylidene difluoride membranes and blots were probed with HAb18 mAb (prepared in our laboratory). Actin was chosen as internal control and the blots were probed with mouse antiactin mAb (Chemicon International, Inc.).

Flow Cytometry

Twenty-four, 48, 72, and 96 h after siRNA transfection, HCC cells were harvested respectively, stained with RPE-labeled anti-CD147 antibody (Serotec) and subjected to flow cytometric analysis using a FACSCalibur flow cytometer (Becton Dickinson) and CellQuest software (Becton Dickinson).

Gelatin Zymography

Forty-eight hours after siRNA transfection, conditioned medium was collected and separated by 8% acrylamide gels containing 0.1% gelatin. The gels were incubated in 2.5% Triton X-100 solution at room temperature with gentle agitation and then were soaked in reaction buffer [0.05 mol/L Tris-HCl (pH 7.5), 0.2 mol/L NaCl, and 0.01 mol/L CaCl₂] at 37°C overnight. After reaction, the gels were stained for 6 h and were destained for ~0.5 h. To detect the efficacy of HAb18 mAb, 5 μg/5 μL HAb18 mAb, 5 μg/5 μL anti-JEV mAb (mouse, IgG, kindly provided by the Department of Microorganism, Fourth Military Medical University; negative control), or free-serum medium (blank) was added to the HCC cells for 24-h incubation. Then, the conditioned medium was collected and analyzed as described above.

In vitro Invasion Assays

The assay was done by using chambers with polycarbonate filters (pore size, 8 μm) coated on the upper side with Matrigel (Becton Dickinson Labware). Twenty-four hours after siRNA transfection, HCC cells were harvested and 1×10^5 transfected cells alone or together with equal fibroblasts in 300 μL of 0.1% serum medium were placed in the upper chamber. The snc-RNA–transfected cells were used as negative control. The lower chamber was filled with 0.1% fetal bovine serum medium (200 μL) and serum-free conditioned medium from fibroblasts (200 μL). After 24-h incubation and removal of the cells on the

Table 1. Number of Mice with Metastasis in Each Group

No. Metastasis in Each Mouse	Blank Control, *n* (%)	Negative Control, *n* (%)	HAb18*, *n* (%)	LICARTIN (Low) [†], *n* (%)	LICARTIN (High) [‡], *n* (%)
0	0 (0.00)	0 (0.00)	9 (75)	6 (85.71)	7 (100.0)
<50	5 (41.67)	2 (28.57)	1 (8.33)	1 (14.29)	0 (0.00)
>50	7 (58.33)	5 (71.43)	2 (16.67)	0 (0.00)	0 (0.00)
Total	12	7	12	7	7

NOTE: $P < 0.001$ among the five groups, $\alpha = 0.05$, compared with negative control group.
*$P = 0.003$, corrected $\alpha' = 0.005$.
[†]$P = 0.001$, corrected $\alpha' = 0.005$.
[‡]$P = 0.001$, corrected $\alpha' = 0.005$.
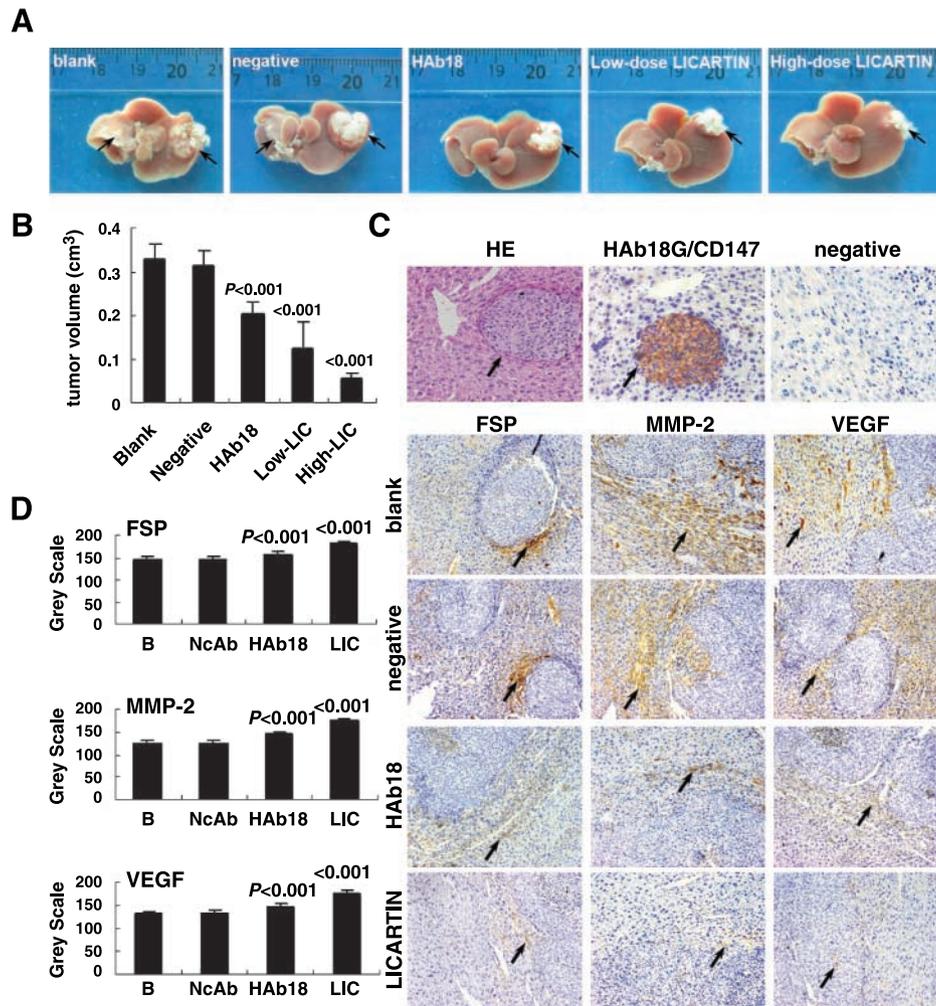
FIGURE 5. HAb18 mAb and LICARTIN treatments inhibited tumor growth, metastasis, and the expression of FSP, MMP-2, and VEGF in HCC microenviroment in a nude mice model. **A.** One month after the HAb18 mAb or LICARTIN treatment, the tumor size of the implanted HCC (*right arrow*) was measured in the resected liver. The metastases could be observed in the blank and negative control groups (*left arrow*). **B.** Quantitative analysis data of tumor volume in the five groups. Columns, mean from all the mice; bars, SD. *P* value of treated group versus negative control group was given in the figure. **C.** Tumor histology. HE, H&E staining shows the metastasized tumors (*arrow*). HAb18G/CD147, expression of HAb18G/CD147 was examined by immunohistochemistry developed with HAb18 mAb. Positive staining (*brown, arrow*) is shown in the metastasized tumor. FSP, MMP-2, and VEGF, expression of FSP, MMP-2, and VEGF in the liver of nude mice 1 mo after treatments. FSP positively stained cells distributed as clusters around the implanted tumors and metastases. The expression of MMP-2 was mainly detected in the stroma, whereas the expression of VEGF on the vascular endothelial cells and in the stroma. The sections were photographed using a ×10 objective on an Olympus BH2 microscope. **D.** Gray scale analyses of the positive staining intensity in the images from each mouse were done by computer image analyzer (Leica Q570c). The stronger the positive staining was, the lower the gray scale value would be. The *P* value of the treated group versus negative control group was given in the figure.

upper chamber of the filter with a cotton swab, the cells on the underside were fixed, stained, and counted. To investigate the inhibitory effects of HAb18 mAb, the upper chamber was filled with 10 μg HAb18 mAb, 10 μg anti-JEV mAb (negative control), or 0.9% NaCl solution (blank).

Competitive Binding Tests

The HCC cells in exponential phase of growth were harvested. Cells (5×10^5) in 300 μL of PBS were incubated with HAb18 mAb 2.5 μg for 30 min. After washing twice with PBS, 2.5 μL RPE-labeled anti-CD147 antibody (Serotec) was added for 20-min incubation in dark. The blank control cells were only incubated with PBS and the positive ones with RPE-labeled anti-CD147 antibody (Serotec). After washing, the cells were detected for fluorescent staining by flow cytometry as described above.

Cell Growth Tests

HCC cells were cultured in 96-well plate (6×10^3 per well) for 8 h, followed, respectively, by anti-JEV mAb (1 μg/well, negative control), HAb18 mAb (1 μg/well), ^{131}I (1.85 MBq/well), and LICARTIN (1.85 MBq/well) treatment in the appropriate wells. Medium was added in the blank control cells. Each condition was triplicated. After 1-h incubation, cells were washed thrice with fresh medium and cultured at 37°C, 5% CO_2. Cells were harvested and counted every day. The doubling time (T) was calculated according to the formula $T = t \times \log 2 / (\log N_t - \log N_0)$. N_t means the cell number

after cultured t hours, N_0 means the cell number at the beginning of the culture, and t means the culture time.

Establishment of Orthotopic Model of HCC in Nude Mice and Animal Studies

We chose orthotopic model of HCC in nude mice for the primary tumor can form in a microenvironment close to the one it originated from (33). The BALB/c nude mice bearing MHCC97-H were supplied by Liver Cancer Institute of Fudan University (Shanghai, China). The mice were sacrificed and the tumors were resected under aseptic conditions, put into MEM medium with 0.1% FBS, cut to 1 mm^3, and then implanted under the liver capsule of left hepatic lobe of BALB/c nude mice. The animals were randomized to i.v. treated with 10 mg/kg anti-JEV mAb [once daily, 8 days, negative control, the number of mice (n) = 7], 10 mg/kg HAb18 mAb (once daily, 8 days, n = 12), 93.5 MBq/kg (n = 7), or 187 MBq/kg LICARTIN (given at the 1st, 4th, and 8th days, n = 7), or 0.2 mL 0.9% NaCl solution (blank control, given at the 1st, 4th, and 8th days, n = 12), beginning from the 1st day postimplantation. The general state of health was observed every day and the mice were weighed every other day. The mice were sacrificed 1 month after the implantation and the tumors from each mouse were removed. Tumor size was measured and tumor volume was determined using the formula $(LW^2) / 2$, where L is the maximum diameter of the tumor and W is the perpendicular diameter of the tumor. Inhibitory rates of tumor growth were calculated using the formula $1 -$ (posttreatment tumor volume of treated group $- 1$) / (posttreatment tumor volume of negative control group $- 1$) $\times$ 100%.

The main organs, including the heart, liver, spleen, lung, kidney, stomach, and intestines were excised and the metastases were counted and the mesenteric lymph nodes were also examined. Then, the above tissues of all the mice were fixed and embedded in paraffin and serially sectioned at a thickness of 4 μm. H&E staining was done to verify the metastasis according to the morphologic characteristics, respectively, by two individual pathologists. Animal studies were approved by the local regulatory agency (Laboratory Animal Research Centre of the Fourth Military Medical University).

Immunohistochemistry

The analysis was developed, respectively, with HAb18 mAb (1:500 diluted), rabbit anti–MMP-2 (Boster), rabbit anti-VEGF (Boster), and rabbit anti-FSP (Boster) as primary antibody using Histostain TM SP kits (Zymed) according to the manufacturer's instructions. The negative control was established at the same time.

Statistical Analysis

Each *in vitro* quantitative tests were independently replicated and the data were calculated as mean ± SD. One-way ANOVA and multiple comparison were used to compare the MMP production, trans-filter cell number, body weight of nude mice, tumor size, and gray value of immunohistochemistry staining in different groups. Compar-

ison of inhibitory effects on MMP secretion and cell invasion between HAb18G/CD147 silence and MMPs silence was done with χ^2 analysis. The univariate ANOVA was used to analyze the growth of HCC cells in different groups. Tumor metastasis in different groups was analyzed with Kruskal-Wallis test and Mann-Whitney test. The above analyses were done using SPSS 11.5 statistical software. All statistical tests were two-sided and P values <0.05 were considered statistically significant, except that for Mann-Whitney Test, corrected $\alpha' = 0.005$ was used and P values <0.005 were considered statistically significant.

References

1. Bhowmick NA, Moses HL. Tumor-stroma interactions. Curr Opin Genet Dev 2005;15:97–101.

2. Liotta LA, Kohn EC. The microenvironment of the tumour-host interface. Nature 2001;411:375–9.

3. Egeblad M, Werb Z. New functions for the matrix metalloproteinases in cancer progression. Nat Rev Cancer 2002;2:161–74.

4. Tang Y, Kesavan P, Nakada MT, Yan L. Tumor-stroma interaction: positive feedback regulation of extracellular matrix metalloproteinase inducer (EMMPRIN) expression and matrix metalloproteinase-dependent generation of soluble EMMPRIN. Mol Cancer Res 2004;2:73–80.

5. Toole BP. Emmprin (CD147), a cell surface regulator of matrix metalloproteinase production and function. Curr Top Dev Biol 2003;54:371–89.

6. Gabison EE, Hoang-Xuan T, Mauviel A, Menashi S. EMMPRIN/CD147, an MMP modulator in cancer, development and tissue repair. Biochimie 2005;87:361–8.

7. Polette M, Gilles C, Marchand V, et al. Tumor collagenase stimulatory factor (TCSF) expression and localization in human lung and breast cancers. J Histochem Cytochem 1997;45:703–9.

8. Muraoka K, Nabeshima K, Murayama T, Biswas C, Koono M. Enhanced expression of a tumor-cell-derived collagenase stimulatory factor in urothelial carcinoma: its usefulness as a tumor marker for bladder cancers. Int J Cancer 1993;55:19–26.

9. Sameshima T, Nabeshima K, Toole BP, et al. Expression of Emmprin (CD147), a cell surface inducer of matrix metalloproteinases, in normal human brain and gliomas. Int J Cancer 2000;88:21–1.

10. Kanekura T, Chen X, Kanzaki T. Basigin (CD147) is expressed on melanoma cells and induces tumor cell invasion by stimulating production of matrix metalloproteinases by fibroblasts. Int J Cancer 2002;99:520–8.

11. Bordador LC, Li X, Toole B, et al. Expression of Emmprin by oral squamous cell carcinoma. Int J Cancer 2000;85:347–52.

12. Nabeshima K, Suzumiya J, Nagano M, et al. Emmprin, a cell surface inducer of matrix metalloproteinases (MMPs), is expressed in T-cell lymphomas. J Pathol 2004;202:341–51.

13. Chen ZN, Liu YF. Monoclonal antibody HAb18 to human hepatoma. Monoclonal Antibodies 1990;8:11.

14. Liu YF, Chen ZN, Ji YY. Localization of hepatocellular carcinoma with monoclonal antibodies. Zhonghua Yi Xue Za Zhi 1991;71:362–5.

15. Chen ZN, Xing JL, Zhang SH, inventors; NTD patent & trademark agency Ltd., Beijing office, assignee. Anti-human hepatoma monoclonal antibody HAb18 light/heavy chain variable region gene, and use thereof. Chinese patent ZL02114471.0, 2002 March 15; PCT international patent WO03/078469; 2003 March 17.

16. Chen ZN, Shang P, Li Y, Qian AR, Zhu P, Xing JL, inventors; NTD patent & trademark agency Ltd., Beijing office, assignee. HAb18G/CD147, its agonist and application. Chinese patent ZL01131735.3, 2001 Sep 28; PCT international patent WO02/094875; 2002 May 27.

17. Zhang Q, Zhou J, Ku XM, et al. Expression of CD147 as a significantly unfavorable prognostic factor in hepatocellular carcinoma. Eur J Cancer Prev 2007;16:196–202.

18. Zhang Q, Chen XG, Zhou J, et al. CD147, MMP-2, MMP-9 and MVD-CD34 are significant predictors of recurrence after liver transplantation in hepatocellular carcinoma patients. Cancer Biol Ther 2006;5:808–14.

19. Chen ZN, Mi L, Xu J, et al. Targeting radioimmunotherapy of hepatocellular carcinoma with iodine (^{131}I) Metuximab injection: clinical phase I/II trials. Int J Radiat Oncol Biol Phys 2006;65:435–44.

20. Chen ZN, Liu YF, Jiang MD, Deng JL, Sui YF. Radiolocalization of human hepatoma with anti-human hepatoma monoclonal antibodies and its F(ab')$_2$ in tumor-bearing nude mice. Zhonghua Yi Xue Za Zhi 1989;69:566–8.

21. Zhang Z, Bian HJ, Feng Q, et al. Biodistribution and localization of iodine-131 labeled Metuximab in patients with hepatocellular carcinoma. Cancer Biol Ther 2006;5:318–22.

22. Xu J, Shen ZY, Chen XG, et al. A randomized controlled trial of Licartin for preventing hepatoma recurrence after liver transplantation. Hepatology 2007;45: 269–76.

23. Lou CY, Feng YM, Qian AR, et al. Establishment and characterization of human hepatocellular carcinoma cell line FHCC-98. World J Gastroenterol 2004; 10:1462–5.

24. Tian J, Tang ZY, Ye SL, et al. New human Hepatocellular carcinoma (HCC) cell line with highly metastatic potential (MHCC97) and its expressions of the factors associated with metastasis. Brit J Cancer 1999;81:814–21.

25. Jiang JL, Zhou Q, Yu MK, Ho LS, Chen ZN, Chan HC. The involvement of HAb18G/CD147 in regulation of store-operated calcium entry and metastasis of human hepatoma cells. J Biol Chem 2001;276:46870–7.

26. Huang Y, Jiang JL, Dou KF, Chen ZN. HAb18G/CD147 enhances the secretion of matrix metalloproteinases (MMP) via cGMP/NO-sensitive capacitative calcium entry (CCE) and accordingly attenuates adhesion ability of fibroblasts. Eur J Cell Biol 2005;84:59–73.

27. Jiang JL, Chan HC, Zhou Q, et al. HAb18G/CD147-mediated calcium mobilization and hepatoma metastasis require both C-terminal and N-terminal domains. Cell Mol Life Sci 2004;61:2083–91.

28. Chung TW, Moon SK, Chang YC, et al. Novel and therapeutic effect of caffeic acid and caffeic acid phenyl ester on hepatocarcinoma cells: complete regression of hepatoma growth and metastasis by dual mechanism. FASEB J 2004;18:1670–81.

29. Yang JM, O'Neill P, Jin W, et al. Emmprin (CD147) confers resistance of breast cancer cells to anoikis through inhibition of bim. J Biol Chem 2006;281: 9719–27.

30. Zucker S, Cao J, Chen WT. Critical appraisal of the use of matrix metalloproteinase inhibitors in cancer treatment. Oncogene 2000;19:6642–50.

31. Bramhall SR, Rosemurgy A, Brown PD, Bowry C, Buckels JA; Marimastat Pancreatic Cancer Study Group. Marimistat as first-line therapy for patients with unresectable pancreatic cancer: A randomized trial. J Clin Oncol 2001;19: 3447–55.

32. Moore MJ, Hamm P, Eisenberg P, Dagenais M, Hagan K, Fields A. A comparison between gemcitabine and the matrix metalloproteinase inhibitor BAY 12-9566 in patients with advanced pancreatic cancer. Proc Am Soc Clin Oncol 2000;19:240a.

33. Maria P, Stanley Z. Matrix metalloproteinase inhibitors (MMPIs): the beginning of phase I or the termination of phase III clinical trials. Cancer Metastasis Rev 2003;22:177–203.

34. Hess KR, Abbruzzese JL. Matrix metalloproteinase inhibition of pancreatic cancer: matching mechanism of action to clinical trial design. J Clin Oncol 2001; 19:3445–6.

35. Chen X, Su Y, Fingleton B, et al. Increased plasma MMP9 in integrin α_1-null mice enhances lung metastasis of colon carcinoma cells. Int J Cancer 2005;116: 52–61.

HAb18G/CD147 Functions in Invasion and Metastasis of Hepatocellular Carcinoma

Jing Xu, Hui-Yun Xu, Qing Zhang, et al.

Updated version	Access the most recent version of this article at: http://mcr.aacrjournals.org/content/5/6/605

Cited articles	This article cites 33 articles, 5 of which you can access for free at: http://mcr.aacrjournals.org/content/5/6/605.full#ref-list-1
Citing articles	This article has been cited by 8 HighWire-hosted articles. Access the articles at: http://mcr.aacrjournals.org/content/5/6/605.full#related-urls

E-mail alerts	Sign up to receive free email-alerts related to this article or journal.
Reprints and Subscriptions	To order reprints of this article or to subscribe to the journal, contact the AACR Publications Department at pubs@aacr.org.
Permissions	To request permission to re-use all or part of this article, use this link http://mcr.aacrjournals.org/content/5/6/605. Click on "Request Permissions" which will take you to the Copyright Clearance Center's (CCC) Rightslink site.